Edge Enhancement in X-Ray Parametric Down Conversion

[1]B. W. Adams, [2]E.M. Dufresne
[1]Argonne National Laboratory, Argonne, IL, USA
[2]University of Michigan, Ann Arbor, MI, USA

Introduction

Parametric down conversion (PDC) is the effect of a spontaneous decay of a photon ("pump") into a pair of highly correlated photons ("signal" and "idler"). The effect is well known in laser physics and has been predicted [1] and demonstrated [2, 3, 4, 5, 6] for x-rays, as well. It can be described semiclassically as the four-wave mixing of the pump-photons with vacuum fluctuations, producing the signal and idler photons. A nonlinear optical medium is required, which also has to support the matching of the wave vectors of the participating photons. With x-rays, the nonlinearity is due to higher-order corrections of Thomson scattering from free, or weakly bound electrons [2, 7], which are due to the Lorentz force and a nonlinear displacement current. This nonlinearity is very small, and processes such as harmonic generation are most probably out of the question at 3rd generation x-ray sources. Due to the high virtual power density of the electromagnetic vacuum fluctuations at x-ray frequencies, PDC is observable with some effort. The same level of observability in an effect based only upon real x-ray photons would be reached with a source that has a photon degeneracy of the order of one. Current 3rd-generation sources are below this threshold by a factor of 10 to 100.

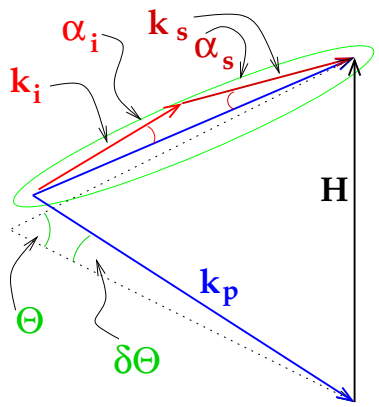

Figure 1: *Wave vector matching in x-ray PDC.*

In all x-ray PDC experiments performed to date, wave vector matching is achieved by diffracting the pump beam in a crystal and detuning slightly away from the Bragg condition, as shown in fig. 1. In the symmetric case $\alpha_i = \alpha_s$ the relation between $\alpha_{i,s}$ and $\delta\Theta$ is [6]

$$\delta\Theta = \frac{\alpha_{i,s}^2/2 + 3\delta}{\sin 2\Theta} \tag{1}$$

where δ is the refractive index decrement. Here (diamond and 23-keV pump photons), $\delta = 1.7 \cdot 10^{-7}$.

Closely associated with PDC is the so-called edge enhancement effect [8]. The observed event rate is proportional to the number of available final states, which depends on the angles $\alpha_{i,s}$ in fig. 1, and thus on the detuning $\Delta\Theta$. This is illustrated in fig. 2: given a detector aperture

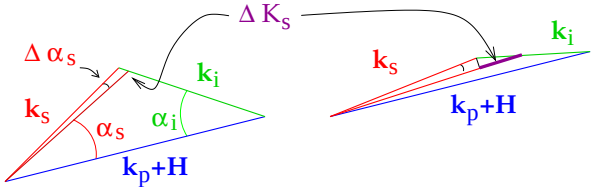

Figure 2: *Edge enhancement in x-ray PDC.*

angle $\Delta\alpha_s$, the range $\mathbf{K}_s \ldots \mathbf{K}_s + \Delta\mathbf{K}_s$ of values admissible for the wave vector $\mathbf{k}_s$ increases as the values of α_i and α_s decrease.

Methods and Materials

The experiment was performed at the MHATT-CAT 7ID beamline of the APS, using a diamond crystal as a nonlinear optical medium. The same crystal had been used in several previous experiments [4, 5] and is described in some detail in [6]. The scattering geometry is shown schematically in fig. 3. X-rays coming from the monochromator on the far left-hand side of the figure are diffracted upward by an InP (220) crystal and enter the diamond crystal, whence they are diffracted into the horizontal direction by the (111) reflection. Thus, the down-converted

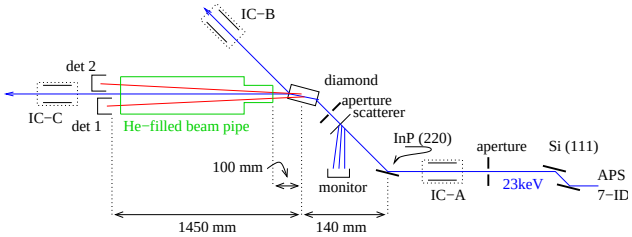

Figure 3: *The scattering geometry*

photons, which exit the diamond at small angles $\alpha_{i,s}$ relative to the diffracted pump beam, are almost horizontal. Two energy-resolving Si drift detectors register these down-converted photons. The ionization chambers shown in the figure were used to determine the flux of pump photons, and thus to obtain a quantitative measure of the conversion event rate. The signals from the two detectors were processed in a multiple, time-resolving multichannel analyzer [9]. This device registers each event in each detector and stores in a computer memory its time of occurence with 20 ns resolution and the photon energy with 256 bit resolution. Correlations, and in particular coincidences, matching energy-dependent selection criteria can then be extracted offline. This capability proved to be very valuable in the present experiment because it made it possible to extract all events for which the energies of the two detected photons added up to that of the pump, regardless of the individual photon energies. In a secondary evaluation step, the energy differences of the coincident photons could then be displayed to show one of the telltale signatures of edge enhancement, namely an increase in the energy bandwidths of the signal and idler photons, of course always adding up to that of the pump.

Results

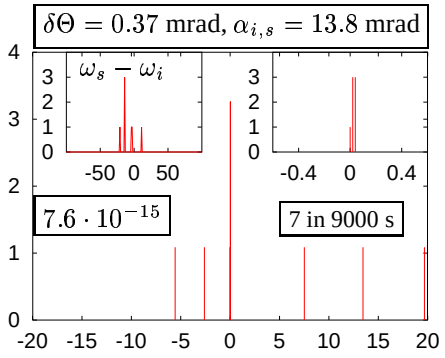

Figure 4: *Time correlation spectrum of energy-selected events in the two detectors and energy differences of the coincident photons (see text).*

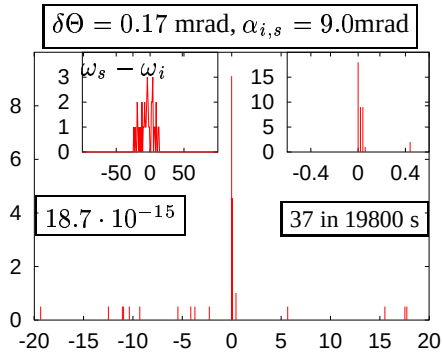

Figure 5: *Same as fig. 4, with* $\delta\Theta = 0.17$ *mrad.*

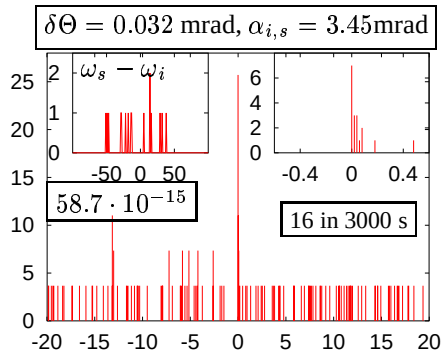

Figure 6: *Same as fig. 4, with* $\delta\Theta = 0.032$ *mrad.*

Figures 4 to 7 show time-correlation spectra of those photons registered in the two detectors that add up to the pump photon energy within $\pm 10\%$ (setting tighter tolerances of $\pm 5\%$ produces very similar results). In all of the figures, the large graph shows the time correlation over $\pm 20\mu$s, the ordinate being scaled in events per 20-ns channel and 10^{15} pump photons; the right-hand insert shows a zoom of the time correlation into the central $\pm 0.5\mu$s, the ordinate being scaled in absolute events per 20-ns channel and the left-hand insert shows the energy

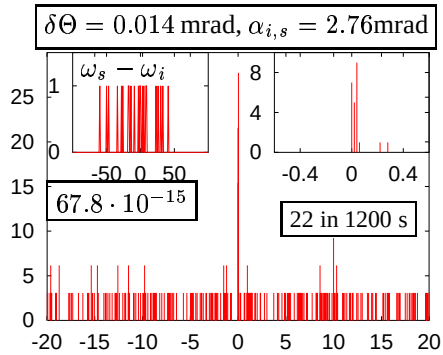

Figure 7: *Same as fig. 4, with* $\delta\Theta = 0.014$ *mrad.*

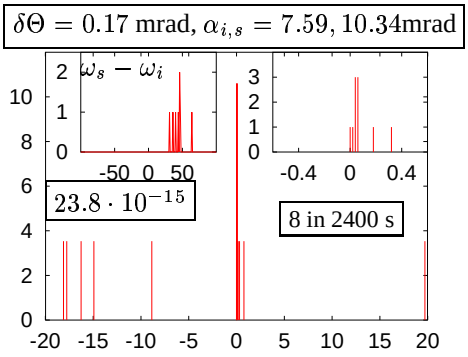

Figure 8: *Asymmetric case (see text).*

differences of the coincident photons (i.e., events in the central peak of the correlation spectrum) in MCA channels (60 eV/channel). The number in the left-hand box gives the coincidence rate per incident pump photon (incident flux determined with the ionization chambers) and the number in the right-hand box gives the number of actual coincidences observed. The four figures 4 to 7 differ in the angles $\alpha_i = \alpha_s$ and corresponding $\delta\Theta$ (by eq. 1). As these angles become smaller, the observed coincidence rate and the energy spread of the down-converted photons increase. Both of these increases are indications of the edge enhancement.

The last figure no. 8 shows the results of an asymmetric configuration with $\alpha_i \neq \alpha_s$. As can be seen by fig. 1, this results in an asymmetric energy splitting ratio between the signal and idler photons.

More on this experiment can be found in ref. [6].

0.1 Conclusion

X-ray parametric down conversion is a weak effect, which can be measured with some experimental effort. Here, quantitative measurements of the conversion event rate are presented, and its angular dependence is demonstrated. Both, the increase in the event rate, and the increase in the energy spread of the down-converted photons are indications of the edge enhancement effect. An asymmetric beam geometry results in an asymmetric energy splitting ratio.

Acknowledgments

Operation of the MHATT-CAT sector 7 beamlines at the Advanced Photon Source was supported by DOE grant No. DE-FG02-99ER45743. Use of the Advanced Photon Source was supported by the U.S. Department of Energy, Office of Science, Office of Basic Energy Sciences, under Contract No. W-31-109-ENG-38.

References

[1] I. Freund and B. Levine, Phys. Rev. Lett. **23**, 854 (1969).

[2] P. Eisenberger and S. McCall, Phys. Rev. Lett. **26**, 684 (1971).

[3] Y. Yoda *et al.*, J. Synchrotron Rad. **5**, 980 (1998).

[4] B. Adams *et al.*, J. Synchrotron Rad. **7**, 81 (2000).

[5] B. Adams *et al.*, Nucl. Instrum. Methods A **467**, 1019 (2001).

[6] in *Nonlinear Optics, Quantum Optics and Ultrafast Pheneomena with x-rays*, edited by B. Adams (Kluwer Acad. Publishers, Boston, 2003), Chap. 5.

[7] in *Nonlinear Optics, Quantum Optics and Ultrafast Pheneomena with x-rays*, edited by B. Adams (Kluwer Acad. Publishers, Boston, 2003), Chap. 3.

[8] D. Kleinman, Phys. Rev. **174**, 1027 (1968).

[9] B. Adams, Rev. Sci. Instrum. **74**, 1128 (2003).